SEMARAK ILMU PUBLISHING

Journal of Advanced Research in Applied Sciences and Engineering Technology

Journal homepage:
https://semarakilmu.com.my/journals/index.php/applied_sciences_eng_tech/index
ISSN: 2462-1943


# Compact Parallel Coupled Line Microstrip BPF Design for 5G Applications

Hardy Ugau Anak Temuli[1], Khairul Najmy Abdul Rani[1, 2,*], Fairul Afzal Ahmad Fuad[1], Khairil Syahmi Musa[1], Norfatihah Bahari[1], Faizah Abu Bakar[1, 2], Mohd Aminudin Jamlos[1, 2], Yusnita Rahayu[3]

[1] Faculty of Electronic Engineering Technology, Universiti Malaysia Perlis, 02100 Padang Besar, Perlis, Malaysia
[2] Advanced Communication Engineering, Universiti Malaysia Perlis, 01000 Kangar, Perlis, Malaysia
[3] Faculty of Engineering, Universitas Riau, 28293 Pekanbaru, Riau, Indonesia

**ARTICLE INFO**

***Article history:***
Received 6 October 2022
Received in revised form 3 November 2022
Accepted 8 December 2022
Available online 4 January 2023

***Keywords:***
Bandpass filter; Fifth generation communications; Insertion loss method; Microstrip; Parallel coupled line filter

**ABSTRACT**

A compact parallel coupled line microstrip bandpass filter (BPF) for sub-6 GHz fifth generation (5G) applications is designed operating between edge frequencies of 3.40 and 3.80 GHz. The design is designed and simulated by means of the Advanced Design System (ADS) software using the flame retardant-4 (FR-4) board as the substrate. The BPF design applies the insertion loss method (ILM) to generate a parallel coupled line filter structure that performs passband permission and unwanted noise attenuation below 3.40 GHz and above 3.80 GHz, respectively. Consistent and relevant performances in terms of matching impedance, return loss (S11), insertion loss (S21), voltage standing wave ratio (VSWR), far field radiation pattern, gain, directivity, and radiated efficiency promise the microstrip BPF design has a potential for sub-6 GHz 5G applications.

## 1. Introduction

Nowadays, many research and developments are performed in the fifth generation (5G) wireless communications to provide high data rate and fulfil the requirement of Gigabit per second (Gbps) to multiple users, simultaneously. Radio frequency (RF) noise is an increasingly critical issue in 5G and wideband radar systems [1]. 5G communications is being implemented widely in 700 Megahertz (MHz), 3.6 Gigahertz (GHz), and 26 GHz bands, respectively. Due to effective rejection of spurious frequencies, microstrip bandpass filter (BPF) is regularly used to filter the RF noise signals and unwanted harmonics [2] whilst defining the operating bandwidth in wireless communication applications [3].

Moreover, BPF with compact size, low loss, and wide passbands becomes highly potential techniques to fulfil the 5G mobile communications requirements [4–5], which includes the massive multiple-input multiple-output (MIMO) system [6]. A BPF consists of several coupled resonators where the dimensions of the distributed lumped elements and number of resonators characterize the BPF [7]. Many miniaturization methods seek to minimize one or other of these quantities.

* *Corresponding author.*
*E-mail address: khairulnajmy@unimap.edu.my*

https://doi.org/10.37934/araset.29.2.3852

As a matter of fact, lumped components are not suitable for very high frequency applications, hence, lumped element of BPF circuit, which is transformed to the planar transmission line circuit is used instead [8]. Recently, many structures and methods have been applied for microstrip line filters, such as combline, hairpin, parallel coupled line, step impedance, and stub impedance [7]. The compact microstrip BPF can be designed using the insertion loss method (ILM) based on network synthesis techniques to obtain a specific type of frequency response. The ILM systematically controls both the passband and stopband amplitude and phase characteristics to synthesize the desired frequency response [9]. In other words, the ILM permits high extents of control over the amplitude, phase and bandpass characteristics with a better way to produce desired response [10]. An ideal BPF design would have zero insertion loss ($S_{21}$), return loss voltage standing wave ratio (VSWR) of one, impedance matching at the desired value (e.g., 50 Ω), and linear phase response in the passband as well as infinite attenuation in the stopband, respectively.

## 2. Design of Parallel Coupled Line Microstrip BPF

Parallel coupled line of microstrip are widely used in microwave component designs, such as microstrip filters including BPF [11], delay lines, impedance matching networks, and directional couplers due to its low-cost fabrication, easy integration [12], more stability [13], and simple design procedure [14]. Figure 1 shows the flowchart of the parallel-coupled line microstrip BPF design. In this paper, a proposed microstrip BPF based on the Butterworth filter response operating frequency between 3.40 and 3.80 GHz is designed and optimized using the Advanced Design System (ADS) software for sub-6 GHz 5G applications.

The ADS software has built-in controllers that can optimize design key parameters for optimum simulated results [15]. The Butterworth filter will generate a maximally flat amplitude response in the passband. The use of maximally flat filter raises contradiction concerns between stability, response time and test precision. Maximally flat filter with low order $N$ has characteristics, such as small filter overshoot, rapid response and bad test precision. High-order maximally flat low-pass filter (LPF) has a good test precision, large overshoot, poor stability, and slow response [16]. In this paper, the BPF design is based on the fourth order ($N$ = 4) maximally flat response.

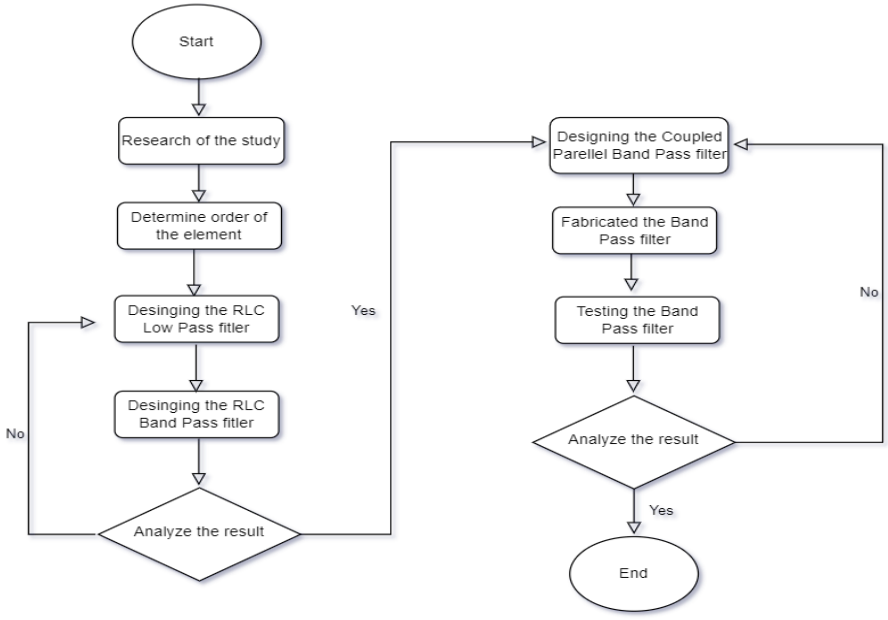


**Fig. 1.** Flowchart of the BPF design

Based on Figure 1, the flowchart starts with the design of a Butterworth LPF then transforms to its respective Butterworth BPF design. In this case, the fourth order ($N$ = 4) LPF is initially designed based on ILM element values as enlisted in Table 1. The LPF has a maximally flat amplitude response in the passband region. Based on Table 1, the 4$^{th}$ order Butterworth maximally flat LPF has elements of $g_1$ = 0.7654, $g_2$ = 1.8478, $g_3$ = 1.8478, and $g_4$ = 0.7654, respectively. Figure 2 shows the lumped element circuit design for the LPF using the ADS software.

**Table 1**
Element values for maximally flat LPF prototype [8]

| $N$ | $g_1$ | $g_2$ | $g_3$ | $g_4$ | $g_5$ | $g_6$ | $g_7$ | $g_8$ | $g_9$ | $g_{10}$ | $g_{11}$ |
|---|---|---|---|---|---|---|---|---|---|---|---|
| 1 | 2.0000 | 1.0000 | | | | | | | | | |
| 2 | 1.4142 | 1.4142 | 1.0000 | | | | | | | | |
| 3 | 1.0000 | 2.0000 | 1.0000 | 1.0000 | | | | | | | |
| 4 | 0.7654 | 1.8478 | 1.8478 | 0.7654 | 1.0000 | | | | | | |
| 5 | 0.6180 | 1.6180 | 2.0000 | 1.6180 | 0.6180 | 1.0000 | | | | | |
| 6 | 0.5176 | 1.4142 | 1.9318 | 1.9318 | 1.4142 | 0.5176 | 1.0000 | | | | |
| 7 | 0.4450 | 1.2470 | 1.8019 | 2.0000 | 1.8019 | 1.2470 | 0.4450 | 1.0000 | | | |
| 8 | 0.3902 | 1.1111 | 1.6629 | 1.9615 | 1.9615 | 1.6629 | 1.1111 | 0.3902 | 1.0000 | | |
| 9 | 0.3473 | 1.0000 | 1.5321 | 1.8794 | 2.0000 | 1.8794 | 1.5321 | 1.0000 | 0.3473 | 1.0000 | |
| 10 | 0.3129 | 0.9080 | 1.4142 | 1.7820 | 1.9754 | 1.9754 | 1.7820 | 1.4142 | 0.9080 | 0.3129 | 1.0000 |

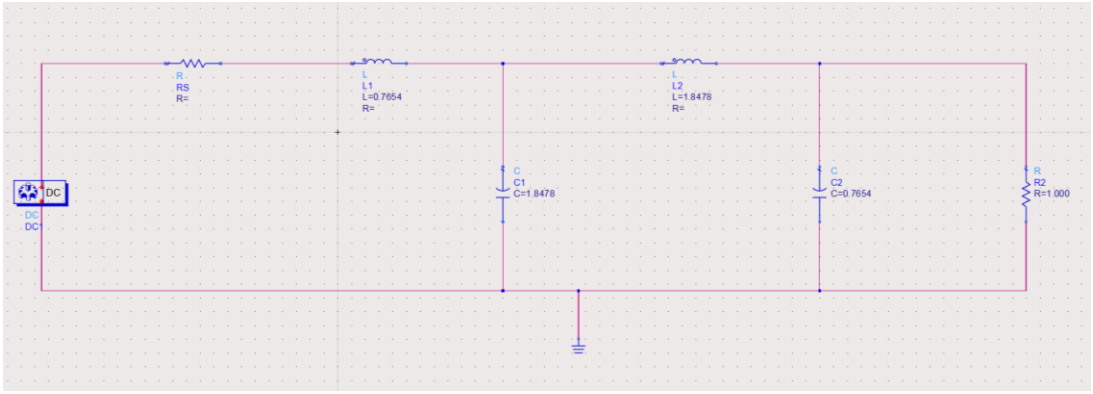


**Fig. 2.** The 4$^{th}$ order butterworth maximally Flat LPF circuit

The conversion of the LPF to the BPF is done systematically based on Figure 3. Basically, each capacitor in the LPF circuit is replaced by parallel inductor and capacitor whereas each inductor in the LPF circuit is replaced by series inductor and capacitor to generate the respective BPF lumped element circuit.

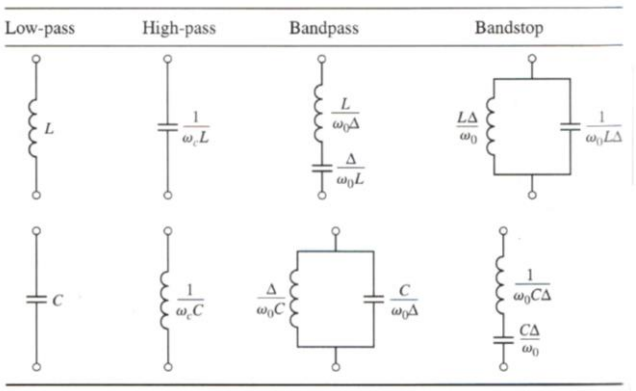


**Fig. 3.** Microwave filter conversion [8]

The equations for BPF transformation are based on Eq. (1) and (2) where the center frequency, $\omega_0$ and fractional bandwidth, $\Delta$ are obtained from the frequency range between $f_1 = 3.4$ GHz and $f_2 = 3.8$ GHz.

$$\omega_0 = \sqrt{\omega_1 \omega_2} \tag{1}$$

where

$$\Delta = \frac{\omega_2 - \omega_1}{\omega_0} \tag{2}$$

Moreover, the series inductor, $L_k$ is transformed to a series resonant (LC) circuit with element values based on Eq. (3) and (4). Furthermore, the shunt capacitor, $C_k$ is transformed to a shunt LC circuit with element values according to Eq. (5) and (6), respectively [17].

$$L_k' = \frac{L_k}{\Delta \omega_0} \tag{3}$$

$$C_k' = \frac{\Delta}{\omega_0 L_k} \tag{4}$$

$$L_k' = \frac{\Delta}{\Delta \omega_0 C_k} \tag{5}$$

$$C_k' = \frac{C_k}{\Delta \omega_0} \tag{6}$$

All the lumped element values of the BPF are calculated with source resistance, $R_0$ = 50 Ω, center frequency, $\omega_0 = 2.2585 \times 10^{10}$ rad/s, and fractional bandwidth, $\Delta = 0.1113$. Figure 4 shows the schematic of the BPF design with all the calculated element values in the ADS software.

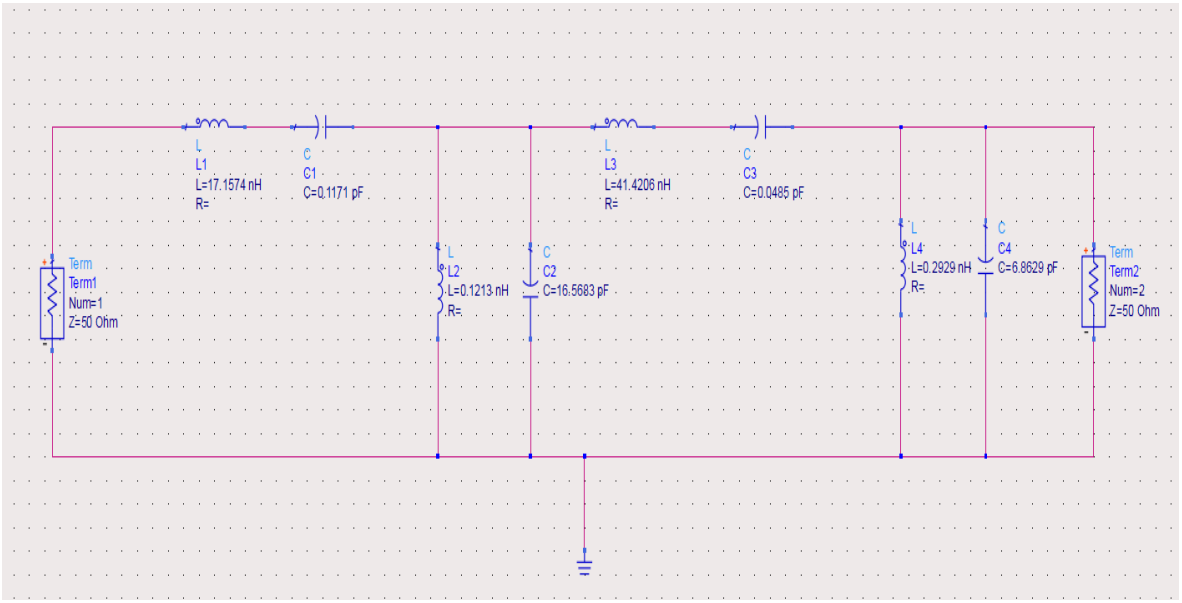


**Fig. 4.** BPF design schematic in the ADS software

Then, there are calculations of odd and even impedance in designing the parallel coupled line BPF. This will determine the width and length of the copper strip of the BPF design. In this case, the odd and even resistances are calculated by using the Eq. (7), (8), and (9) [18].

$$\frac{J_{01}}{Y_0} = \sqrt{\frac{\pi\Delta}{2g_0g_1}} \tag{7}$$

$$\frac{J_{j,j+1}}{Y_0} = \frac{\pi\Delta}{2\sqrt{g_jg_{j+1}}} \tag{8}$$

$$\frac{J_{n,n+1}}{Y_0} = \sqrt{\frac{\pi\Delta}{2g_ng_{n+1}}} \tag{9}$$

Where, $g_0, g_1,$ and $g_{n+1}$ are the elements of ladder type of filter, $J_{j,j+1}$ are the characteristic admittances of $J$ inverters, and $Y_0$ are characteristic admittance of terminating lines. By using the $J$ inverters obtained above, the even and odd type characteristic impedances of the coupled microstrip line resonator are calculated using the Eq. (10) and (11) [18].

$$(Z_{0e})_{j,j+1} = \frac{1}{Y_0}\left[1 + \frac{J_{j,j+1}}{Y_0} + \left(\frac{J_{j,j+1}}{Y_0}\right)^2\right] \tag{10}$$

$$(Z_{0o})_{j,j+1} = \frac{1}{Y_0}\left[1 - \frac{J_{j,j+1}}{Y_0} + \left(\frac{J_{j,j+1}}{Y_0}\right)^2\right] \tag{11}$$

Where $Z_{0e}$ is even characteristic impedance and $Z_{0o}$ is odd characteristic impedance for $j$ equals to 0 to $n$ of elements.

By using the Start LineCalc in the Advanced Design System (ADS) software, the dimensions of width, spacing and length of each stage are calculated by using even and odd characteristic impedances. The characteristic impedance, $Z_0$ is typically assumed to be 50 Ω. The filter is constructed on the FR-4 substrate with a dielectric constant, $\varepsilon_r = 4.60$ and a thickness of 1.57 mm. The FR4 substrate is known of of its small size and lightweight [19]. The effective dielectric constant the substrate is calculated using the Eq. (12) [20].

$$\varepsilon_{reff} = \frac{\varepsilon_r+1}{2}\frac{\varepsilon_r-1}{2}\frac{1}{\sqrt{1+12\frac{h}{w}}} \tag{12}$$

where $w$ and $h$ are the microstrip substrate width and thickness, respectively.

The general structure of parallel coupled line microstrip BPF is depicted in Figure 5. In this case, the coupled-line structure is composed of two quasi-Transverse Electric and Magnetic (TEM) modes: even and odd [21]. For an even-mode incitement, both microstrip lines have the same voltage potentials. On contrary, to implement an odd mode, both microstrip lines should have opposite voltage potentials or carry opposite-sign charges. Moreover, the width, length, and gap of each stage in parallel coupled lines is calculated and optimized in the ADS software using both even- and odd-mode characteristic impedance Eq. (10) and (11), respectively. Figure 6 shows the coupled line microstrip BPF structure designed and simulated in the ADS software.

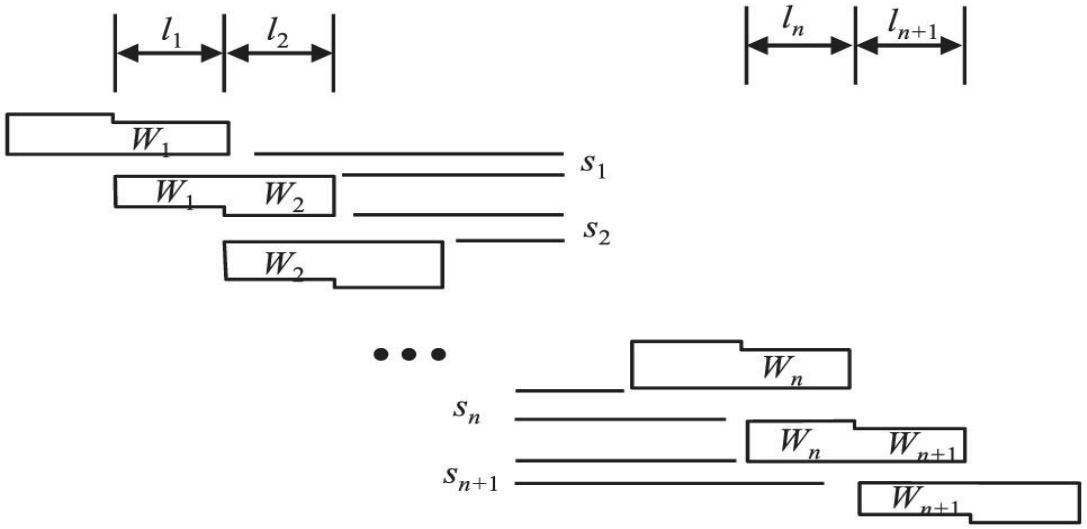


**Fig. 5.** General parallel coupled line microstrip BPF design [2]

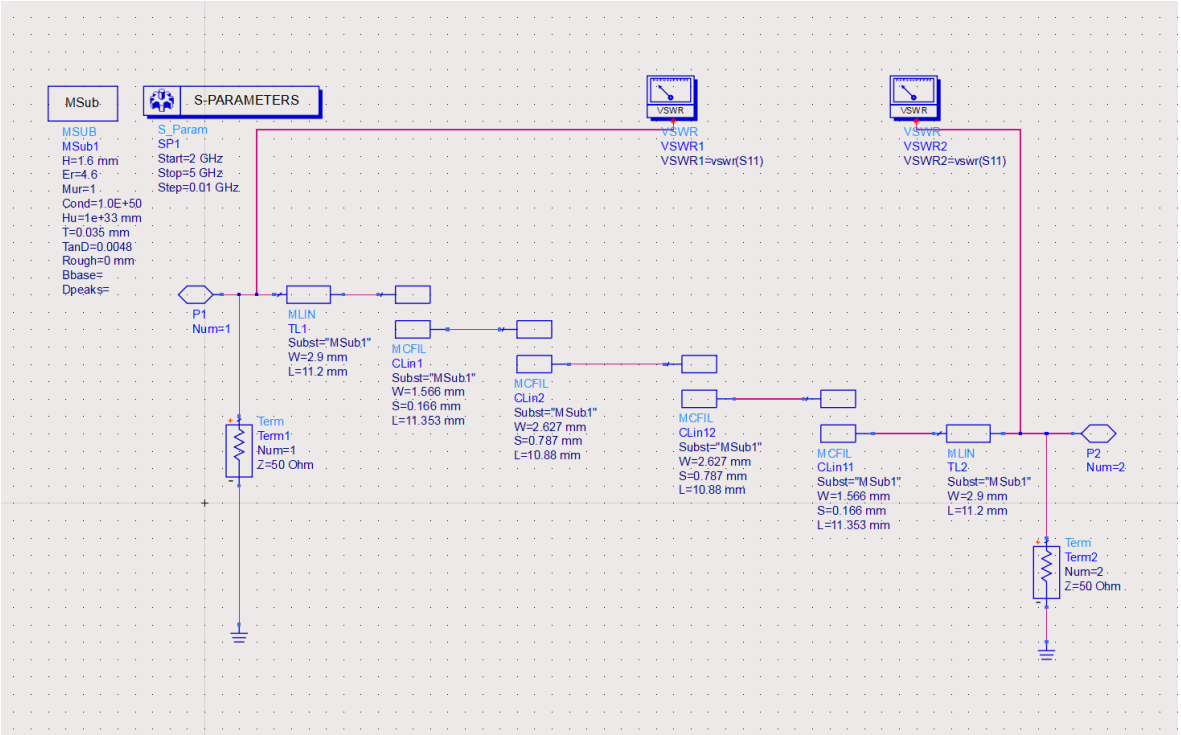


**Fig. 6.** Parallel coupled line microstrip BPF design in the ADS software

Figure 7 shows the respective layout design of the BPF in the ADS software whereas Figure 8 shows the fabricated BPF using the FR-4 substrate with two Sub-Miniature A (SMA) coaxial cable connectors.

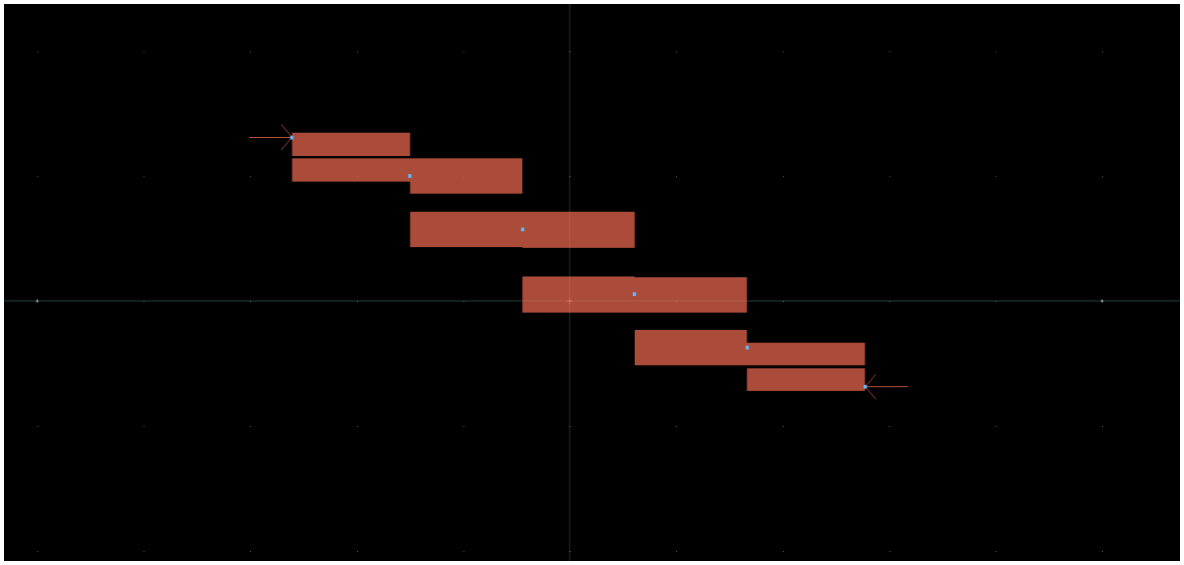

**Fig. 7.** Parallel coupled line microstrip BPF simulation layout in the ADS software

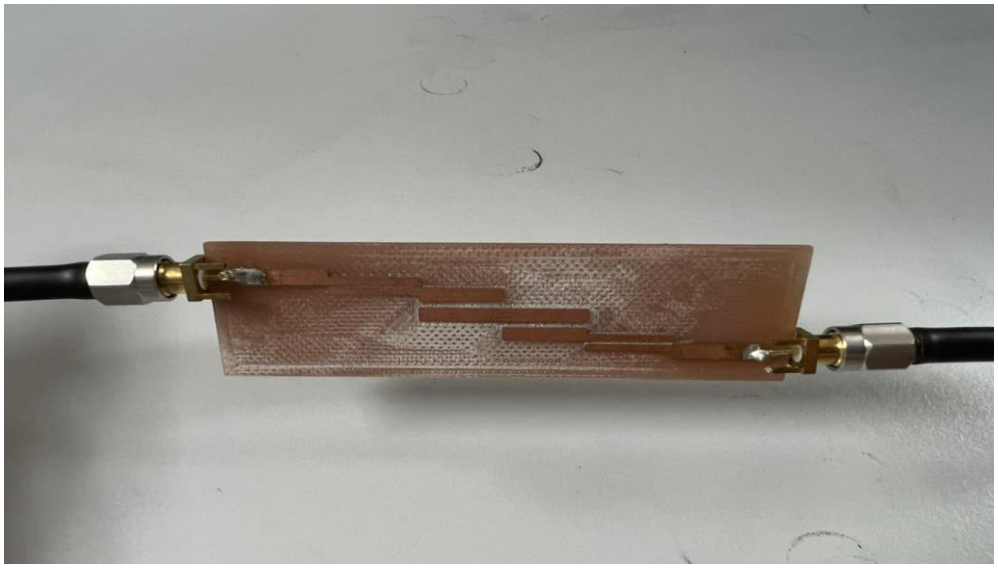

**Fig. 8.** Fabricated BPF design with two SMA ports

## 3. Results

The simulation result of the return loss ($S_{11}$) and insertion loss ($S_{21}$) show that the BPF design operates between 3.423 and 3.766 GHz band edge frequencies as in Figure 9. In this case, the $S_{11}$ is nearly -30 dB at 3.53 GHz whereas $S_{21}$ is -2.007 dB at 3.423 GHz and -2.108 dB at 3.766 GHz, respectively. In this study, the Keysight FieldFox radio frequency (RF) analyzer model N9913A is used to measure the performance of the fabricated BPF. Figure 10 shows the $S_{11}$ of the fabricated BPF is -28.41 dB at 3.53 GHz whereas Figure 11 shows the $S_{21}$ of the fabricated BPF is -13.15 dB at 3.423 GHz and -6.419 dB at 3.766 GHz, respectively.

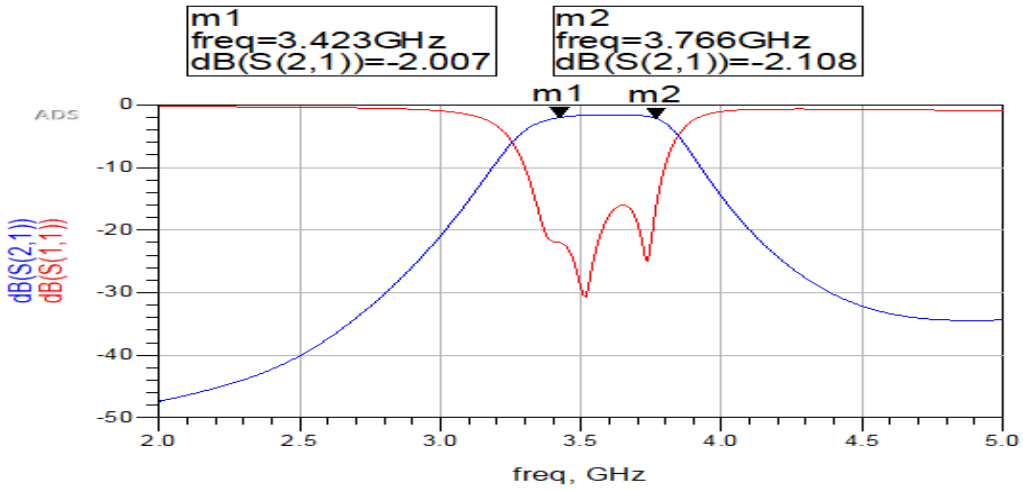


**Fig. 9.** Simulations of return and insertion losses

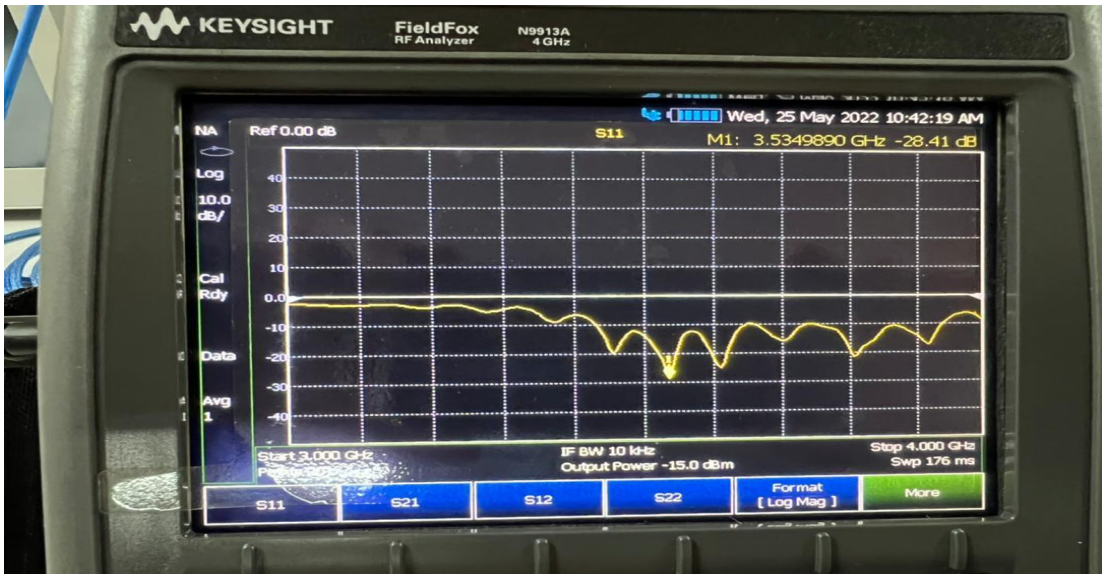


**Fig. 10.** Measurement of return loss

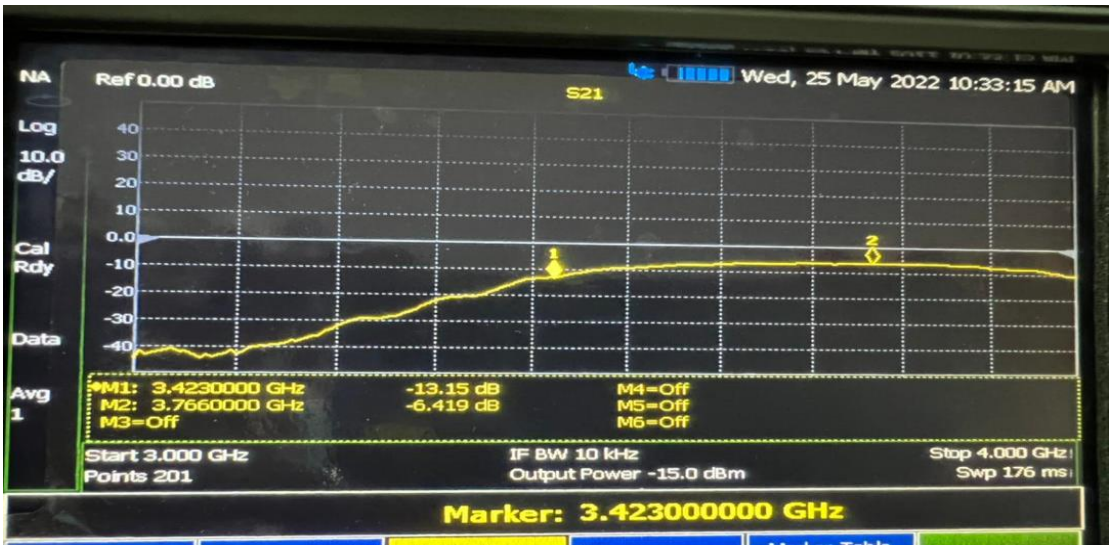


**Fig. 11.** Measurement of insertion loss

Moreover, Figure 12 indicates that return losses ($S_{11}$ and $S_{22}$) have matching impedance nearby 50 Ω within the band edge frequencies. Figure 13 shows the Smith chart plot in which the fabricated BPF has matching impedance close to 50 Ω at the operating frequency of 3.53 GHz. Furthermore, the fabricated BPF has the return loss VSWR of 1.073 as in Figure 14 and return loss phase of 66.88° as in Figure 15 at 3.53 GHz, respectively.

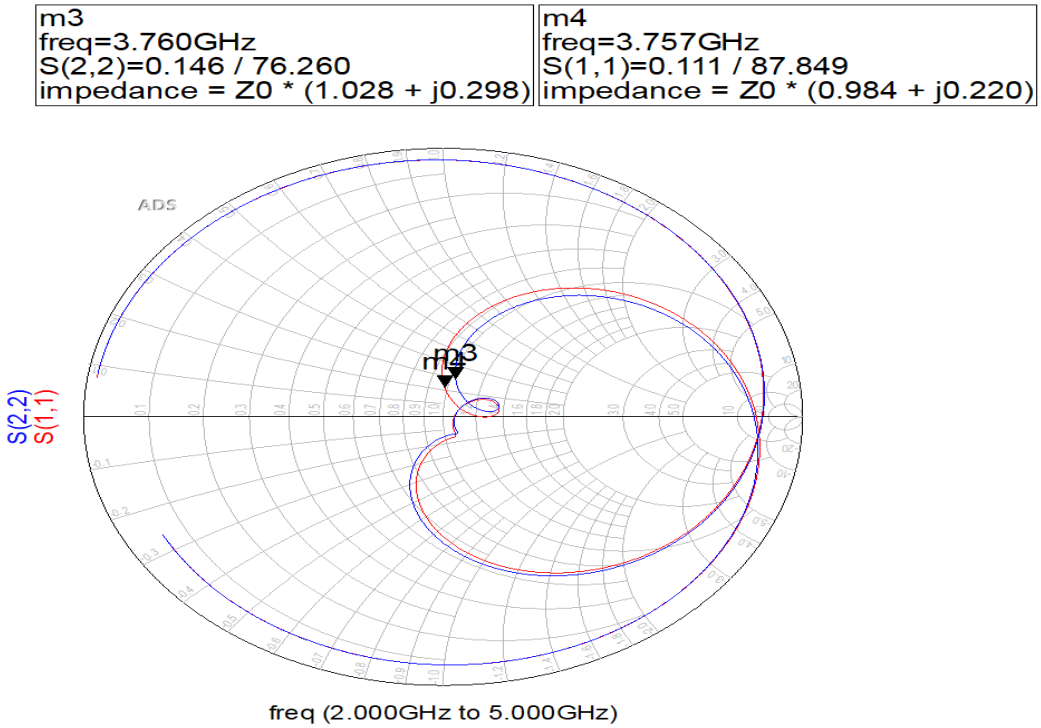


**Fig. 12.** Simulation of return losses with 50 Ω matching impedance


**Fig. 13.** Measurement of return loss with 50 Ω matching impedance

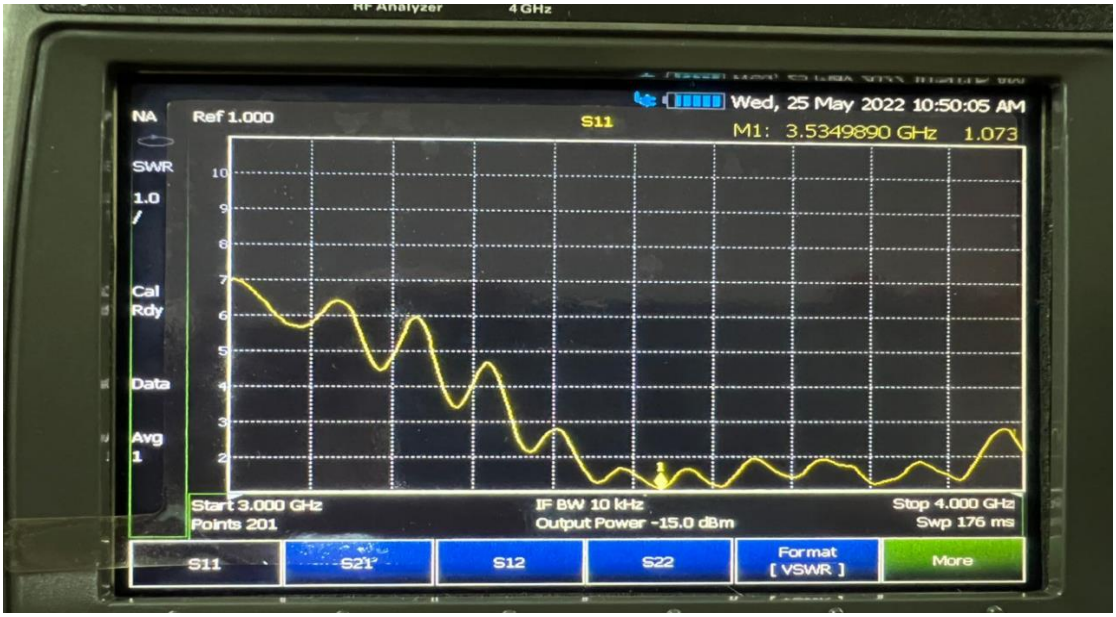


**Fig. 14.** Measurement of Voltage Standing Wave Ratio (VSWR) of return loss

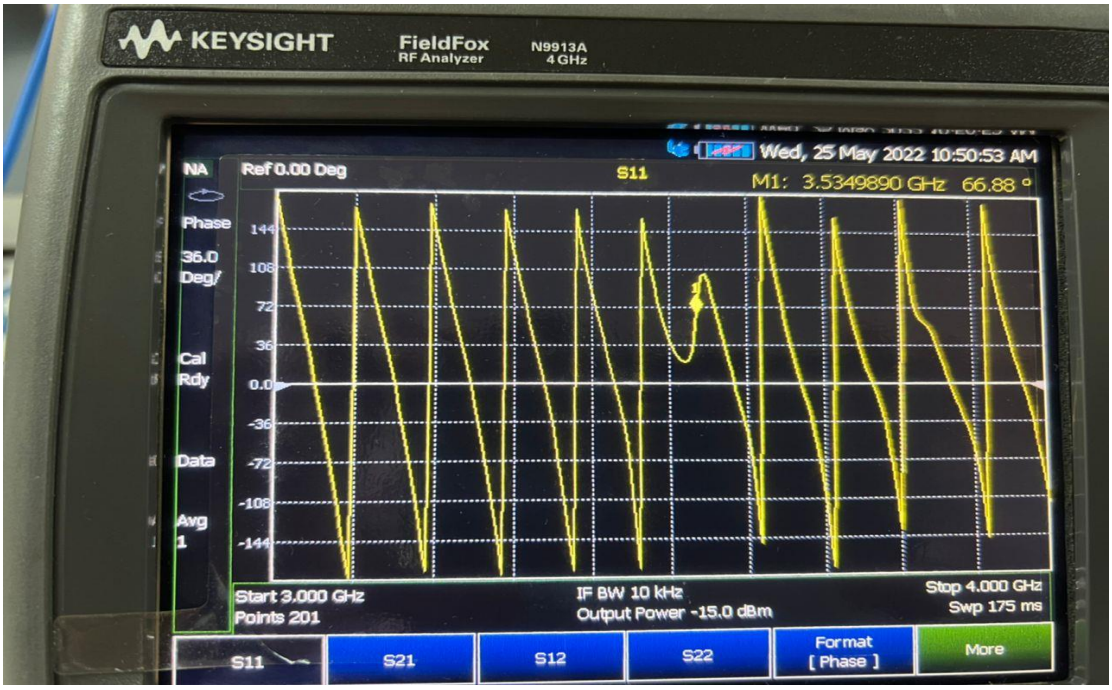


**Fig. 15.** Measurement of phase change of return loss

Far field is a term that refers to a section with normal electromagnetic (EM) radiation at scattering object, such as the BPF. The layout simulation of the BPF far field pattern is shown in Figure 16 for port 1 and Figure 17 for port 2, respectively. On the other hand, radiation pattern represents the variation of the power emitted by an object including the BPF. The simulation of the BPF layout radiation pattern is shown in Figure 18 for port 1 and Figure 19 for port 2, respectively.

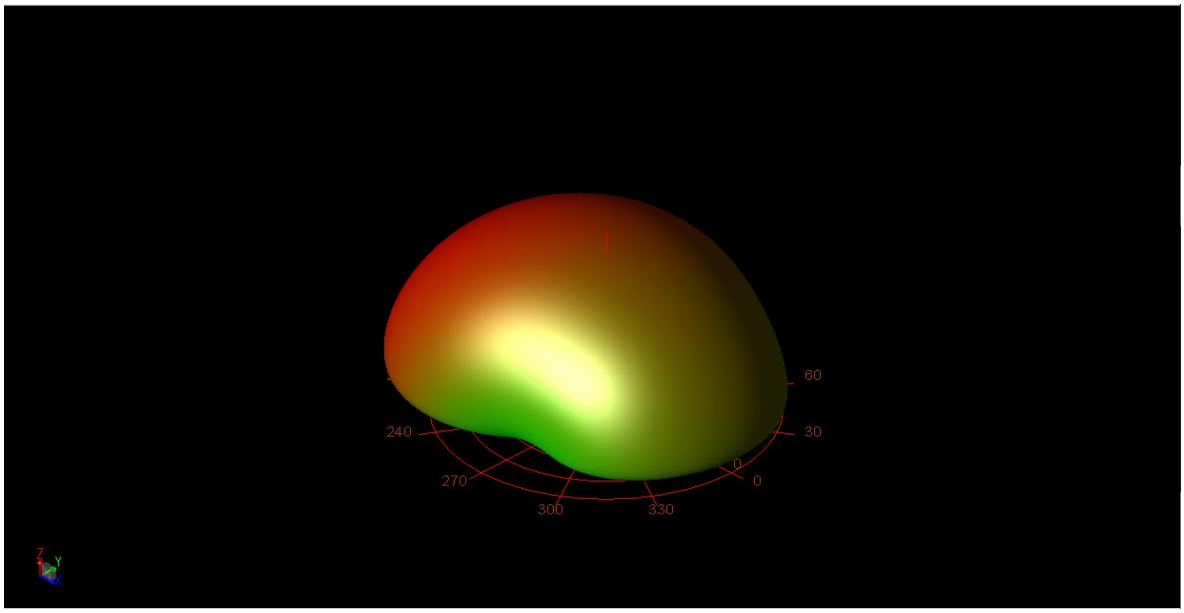


**Fig. 16.** Far field pattern at Port 1 of BPF at 3.40 GHz

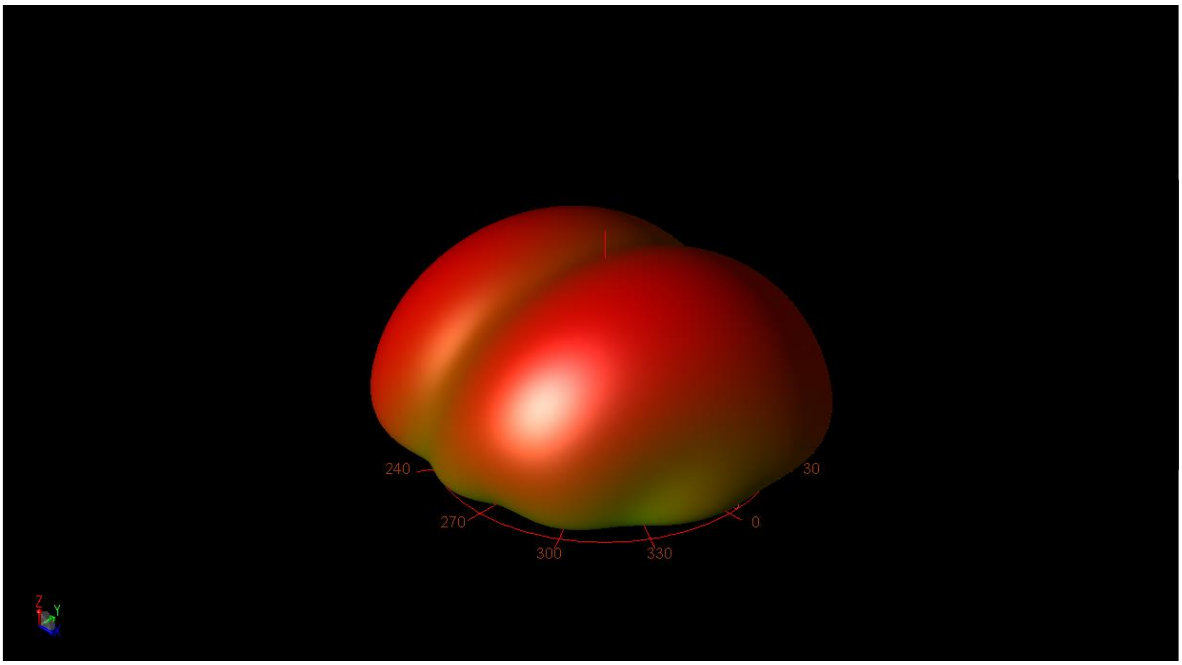


**Fig. 17.** Far field pattern at Port 2 of BPF at 3.80 GHz

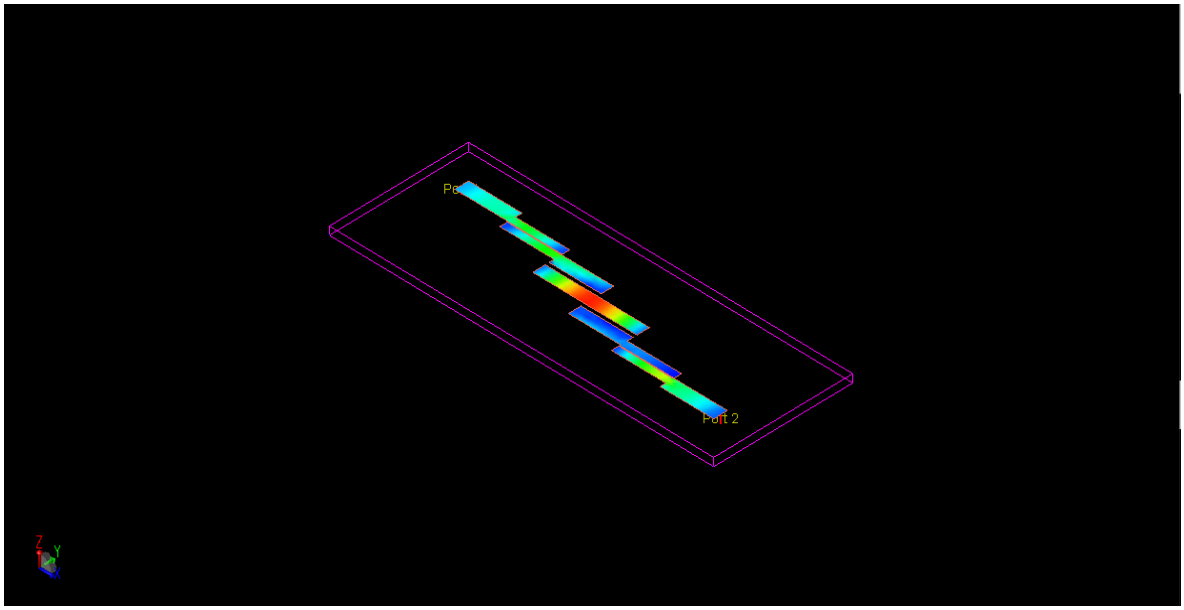


**Fig. 18.** Radiation pattern at Port 1 of BPF

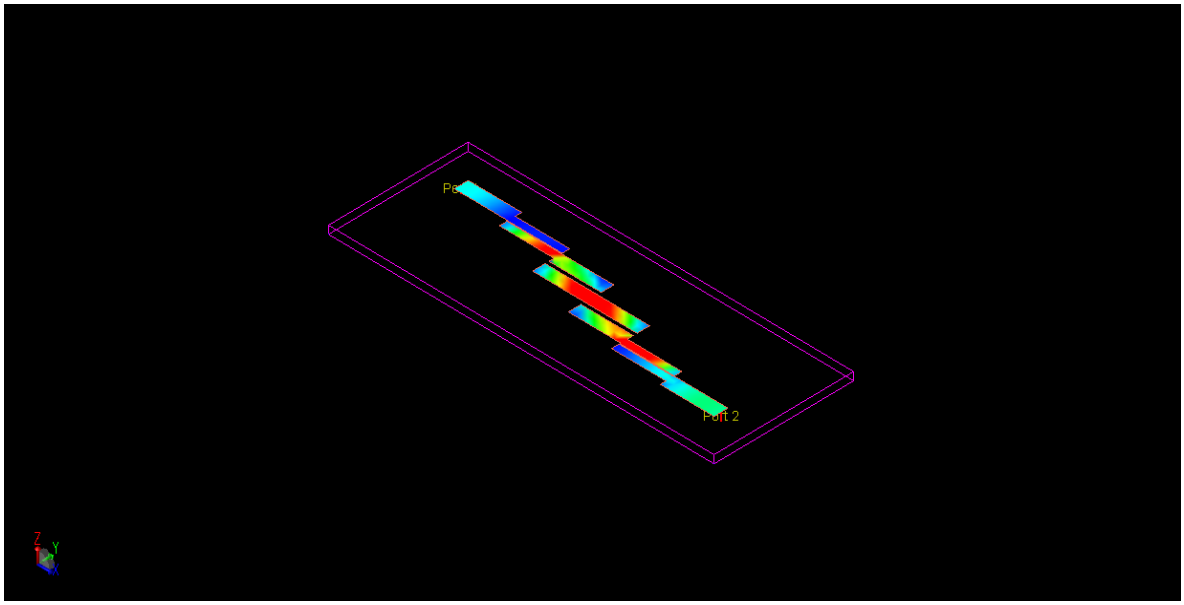


**Fig. 19.** Radiation pattern at Port 2 of BPF

Figure 20 shows the radiated performance parameters for port 1 operating at the lower cut off frequency whereas Figure 21 shows the radiated performance parameters for port 2 operating at the higher cut off frequency, respectively.

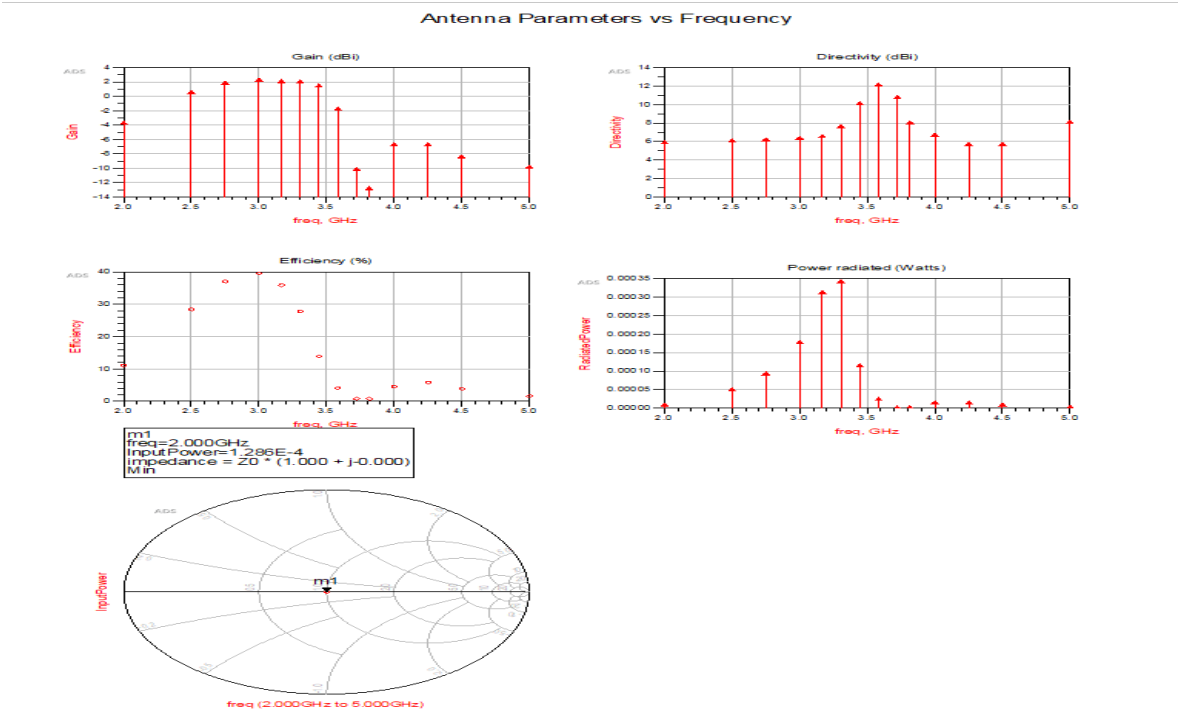


**Fig. 20.** Radiated performance parameters at Port 1 of BPF

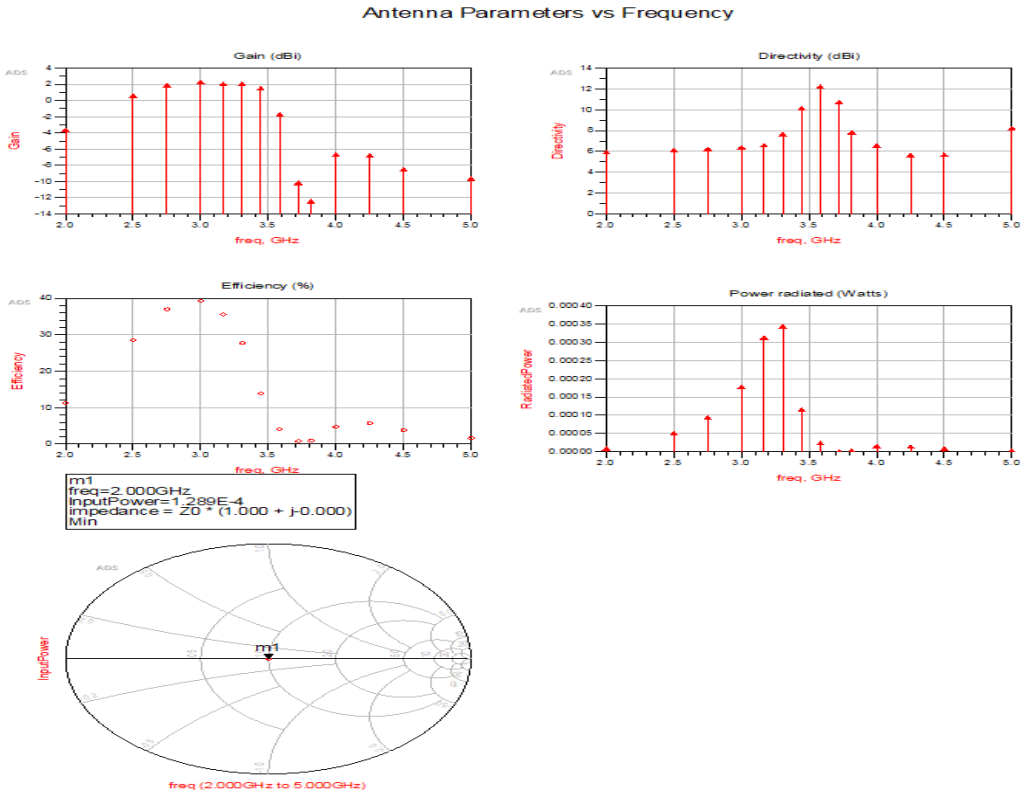


**Fig. 21.** Radiated performance parameters at Port 2 of BP

## 4. Conclusions

In this study, the design of bandpass filter (BPF) using parallel coupled microstrip resonator has been designed and simulated using the ADS software operating at the edge frequencies between

3.40 and 3.80 GHz. The design applies the insertion loss method (ILM) initially based on the 4$^{th}$ order Butterworth maximally flat low-pass filter (LPF) then converted to the respective BPF with the FR4 substrate. The BPF design successfully generates acceptable performance in terms of a good matching impedance of 50 Ω, adequate far field radiation pattern, return loss ($S_{11}$) of below -10 decibel (dB), voltage standing wave ratio (VSWR) near to 1, maximum gain of 1.75 decibel relative to isotropic (dBi), maximum directivity of 10.32 dBi, and maximum radiated efficiency of 13.91 %, respectively. In sum, this parallel coupled line microstrip BPF design can be potentially applied for sub-6 GHz 5G applications.

**Acknowledgement**
Authors are thankful to all colleagues who provided advice and expertise that significantly assisted the paper publication.

**References**

[1] Hussaini, Abubakar S., Yasir I. Abdulraheem, Konstantinos N. Voudouris, Buhari A. Mohammed, Raed A. Abd-Alhameed, Husham J. Mohammed, Issa Elfergani et al. "Green flexible RF for 5G." *Fundamentals of 5G Mobile Networks* (2015): 241-272. https://doi.org/10.1002/9781118867464.ch11

[2] Chen, Chih-Jung. "A coupled-line coupling structure for the design of quasi-elliptic bandpass filters." *IEEE Transactions on Microwave Theory and Techniques* 66, no. 4 (2018): 1921-1925. https://doi.org/10.1109/TMTT.2017.2783378

[3] Hong, Jia-Shen G., and Michael J. Lancaster. *Microstrip filters for RF/microwave applications*. John Wiley & Sons, 2004.

[4] Hou, Zhanyong, Chengguo Liu, Bin Zhang, Rongguo Song, Zhipeng Wu, Jingwei Zhang, and Daping He. "Dual-/Tri-wideband bandpass filter with high selectivity and adjustable passband for 5G mid-band mobile communications." *Electronics* 9, no. 2 (2020): 205. https://doi.org/10.3390/electronics9020205

[5] Shi, Liyun, and Jianjun Gao. "Multitransmission Zero Dual-Band Bandpass Filter Using Nonresonating Node for 5G Millimetre-Wave Application." *Active and Passive Electronic Components* 2018 (2018). https://doi.org/10.1155/2018/7628598

[6] Morshidi, Ummi Haziqah, Dyg Norkhairunnisa Abang Zaidel, Norhudah Seman, Melvin Philip Attan, Dayang Azra Awang Mat, Mohd Ridhuan Mohd Sharip, and Haruichi Kanaya. "Bandwidth Enhancement of 5G Parallel Coupled Line Band Pass Filter Using Patterned Ground Structure Technique." *International Journal of Integrated Engineering* 12, no. 6 (2020): 87-93. https://doi.org/10.30880/ijie.2020.12.06.011

[7] Al-Yasir, Yasir, Raed A. Abd-Alhameed, James M. Noras, Ahmed M. Abdulkhaleq, and N. Ojaroudi Parchin. "Design of very compact combline band-pass filter for 5G applications." (2018): 61-4. https://doi.org/10.1049/cp.2018.1482

[8] Srivastava, Shreyasi, R. K. Manjunath, and P. Shanthi. "Design, simulation and fabrication of a microstrip bandpass filter." *International Journal of Science and Engineering Applications* 3, no. 5 (2014): 154-158.

[9] Thube, Aparna, and Manisha Chattopadhyay. "RF filter design using insertion loss method and genetic optimization algorithm." *International Journal of Engineering Research and Applications* 3, no. 4 (2013): 207-211.

[10] Seghier, Salima, Nasreddine Benahmed, Fethi Tarik Bendimerad, and Nadia Benabdallah. "Design of parallel coupled microstrip bandpass filter for FM Wireless applications." In *2012 6th International Conference on Sciences of Electronics, Technologies of Information and Telecommunications (SETIT)*, pp. 207-211. IEEE, 2012. https://doi.org/10.1109/SETIT.2012.6481915

[11] Chen, Chih-Jung. "Design of parallel-coupled dual-mode resonator bandpass filters." *IEEE Transactions on Components, Packaging and Manufacturing Technology* 6, no. 10 (2016): 1542-1548. https://doi.org/10.1109/TCPMT.2016.2601647

[12] Ding, Dawei, Qingfu Zhang, Jing Xia, Aimin Zhou, and Lixia Yang. "Wiggly parallel-coupled line design by using multiobjective evolutionay algorithm." *IEEE Microwave and Wireless Components Letters* 28, no. 8 (2018): 648-650. https://doi.org/10.1109/LMWC.2018.2848475

[13] Yob, Rashidah Che, Nor Muzlifah Mahyuddin, Mohd Fadzil Ain, Mohd Aminuddin Jamlos, Nur Hidayah Ramli, Norfatihah Bahari, Mohd Wafi Nasrudin, and Liyana Zahid. "Cylindrical Dielectric Resonator as Dielectric Matching on Microwave Amplifier for the Unconditionally Stable and Conditionally Stable Transistor at 5 GHz Frequency." *Journal of Advanced Research in Applied Sciences and Engineering Technology* 29, no. 1 (2022): 30-45.

[14] Kavitha, K., and M. Jayakumar. "Design and performance analysis of hairpin bandpass filter for satellite applications." *Procedia computer science* 143 (2018): 886-891. https://doi.org/10.1016/j.procs.2018.10.366
[15] Embong, ENFS Engku, KN Abdul Rani, and H. A. Rahim. "The wearable textile-based microstrip patch antenna preliminary design and development." In *2017 IEEE 3rd international conference on engineering technologies and social sciences (ICETSS)*, pp. 1-5. IEEE, 2017.
[16] Benjamin, Ayibapreye Kelvin, Priye Kenneth Ainah, and Animiosevbuse Tosan Enoma. "Stepped Impedance Microstrip Lowpass Filter Design using Advanced Design Systems."
[17] Pozar, David M. *Microwave engineering*. John wiley & sons, 2011.
[18] Othman, M. A., M. Sinnappa, M. N. Hussain, M. Z. A. Abd-Aziz, and M. M. Ismail. "Development of 5.8 GHz microstrip parallel coupled line bandpass filter for wireless communication system." *International Journal of Engineering and Technology* 5, no. 4 (2013): 3227-3235.
[19] Zaini, SR Mohd, and KN Abdul Rani. "Wearable inset-Fed FR4 microstrip patch antenna design." In *IOP Conference Series: Materials Science and Engineering*, vol. 318, no. 1, p. 012050. IOP Publishing, 2018. https://doi.org/10.1088/1757-899X/318/1/012050
[20] Kadam, Rajendra N., and A. B. Nandgaonkar. "Design of a Coupled-Line Microstrip Bandpass Filter at 3.5 GHz." *International Research Journal of Engineering and Technology (IRJET)* 2, no. 06 (2015).
[21] Fathi, Esmaeil, Farbod Setoudeh, and Mohammad Bagher Tavakoli. "Design and fabrication of a novel multilayer bandpass filter with high-order harmonics suppression using parallel coupled microstrip filter." *ETRI Journal* 44, no. 2 (2022): 260-273. https://doi.org/10.4218/etrij.2020-0330